RESEARCH ARTICLE
doi: 10.2306/scienceasia1513-1874.2025.081

ScienceAsia 51 (5): 2025: ID 2025081: **1–9**

CEP170 enhances ccRCC progression by promoting platelet aggregation and angiogenesis

Huibing Li[a,b,*], **Shimiao Zhu**[a], **Qi Li**[a], **Zongsu Zhang**[a], **Changyi Quan**[a,*]

[a] Department of Urology, Tianjin Institute of Urology, The Secondary Hospital of Tianjin Medical University, Hexi District, Tianjin 300211 China

[b] Department of Urology, The First Affiliated Hospital and College of Clinical Medicine of Henan University of Science and Technology, Luoyang 471003 China

[*]Corresponding authors, e-mail: researcherlhb@163.com, quanchangyi@tmu.edu.cn

Received 17 May 2025, Accepted 12 Sep 2025
Available online 11 Oct 2025

ABSTRACT: CEP170 (centrosomal protein 170 kDa) is implicated in cancer progression, but its role in clear cell renal cell carcinoma (ccRCC) remains unclear. This study explored how CEP170 drives ccRCC malignancy, revealing its potential as a therapeutic target. Immunoblotting revealed significant upregulation of CEP170 in ccRCC cell lines, while CCK-8 and EdU assays demonstrated that CEP170 silencing suppressed cancer cell proliferation. Functional analyses, including immunostaining, ELISA, and flow cytometry, revealed that CEP170 depletion inhibited platelet aggregation induced by ccRCC cells. Furthermore, tube formation and transwell assays revealed attenuated angiogenesis and migration upon CEP170 knockdown. *In vivo* experiments confirmed that CEP170 silencing hindered tumor growth in mice. Mechanistically, CEP170 activated the Twist1/galectin-3 signaling axis, as validated by immunoblotting, thereby driving platelet aggregation, angiogenesis, and tumor invasion. These findings collectively indicate that CEP170 promotes ccRCC progression by enhancing cancer cell-stimulated platelet aggregation as well as angiogenesis via the Twist1/galectin-3 pathway, highlighting its potential as a target in ccRCC management.

KEYWORDS: renal cell carcinoma, centrosomal protein, platelet aggregation, angiogenesis, Twist1/galectin-3

INTRODUCTION

Clear cell renal cell carcinoma (ccRCC) is a prevalent malignancy worldwide. Owing to advancements in early detection, the mortality rate for ccRCC patients has been gradually decreasing [1]. However, metastasis continues to be the primary cause of death in ccRCC patients [2]. While numerous studies have investigated the mechanisms of metastasis in ccRCC, the exact processes involved remain poorly understood. Platelets play crucial roles in cancer progression by facilitating tumor cell survival, immune evasion, and metastasis through direct interactions and the secretion of protumorigenic factors. In particular, tumor cell-induced platelet aggregation (TCIPA) promotes angiogenesis and facilitates tumor cell adhesion to the vascular endothelium, creating a permissive microenvironment for metastasis. In ccRCC, dysregulated platelet activation has been linked to disease progression and poor prognosis, suggesting that platelet-targeted strategies are potential therapeutic options [3–5]. Pharmacological or genetic inhibition of platelets has been shown to suppress metastasis. Multiple lines of evidence also point to the role of platelet aggregation in ccRCC progression [6]. However, how tumor cells instruct platelets to promote metastasis remain unclear.

CEP170 (centrosomal protein 170 kDa) is a key protein involved in the regulation of centrosome function, cell cycle progression, and multiple cellular processes [7]. It plays a role in maintaining proper centrosome organization and spindle dynamics during cell division [8]. CEP170 has also been implicated in several cancer types, although its specific role in various malignancies is still under investigation [8]. In some cancers, CEP170 has been shown to be upregulated, and its overexpression is associated with increased tumor progression [9]. For example, in prostate cancer, CEP170 overexpression has been linked to increased cell proliferation and resistance to apoptosis [10]. CEP170 expression is correlated with the aggressive behavior of tumor cells, promoting cell migration and invasion in breast cancer [11].

While the role of CEP170 in centrosome function is well established, its potential involvement in platelet–tumor interactions remains unexplored. Given that centrosomal proteins can influence cellular secretion and surface receptor trafficking, we investigated whether CEP170 could modulate platelet activation in ccRCC through these mechanisms. In this study, we explored the role of CEP170 in ccRCC progression. We discovered that CEP170 plays a crucial role in regulating the Twist1/galectin-3 axis, which in turn enhances platelet aggregation as well as angiogenesis in ccRCC cells. These processes contribute to the exacerbation of the malignant phenotype of ccRCC. On the basis of these findings, we propose that CEP170 could serve as a target for ccRCC treatment.

MATERIALS AND METHODS

Cell culture and transfection

The HUVECs (CRL-1730) and ccRCC cell lines, including 786-O (CRL-1932), CaKi-1 (HTB-46), and A-498 (HTB-44), as well as the normal renal cell line HK-2 (CRL-2190), were all purchased from American Type Culture Collection (ATCC, Manassas, USA), maintained in DMEM with 10% FBS, and incubated at 37 °C in a 5% CO_2 incubator. For CEP170 overexpression, the full-length human CEP170 cDNA (NM_014812.5) was cloned. The pcDNA3.1-CEP170 plasmid (2 μg per 1×10^6 cells) was transfected into 786-O cells via Lipofectamine 2000, and stable overexpression was achieved through selection with G418 (800 μg/ml, 14 days). For the knockdown experiments, two specific shRNAs targeting CEP170 were designed: shCEP170#1 (5′-GCAAGATGAAGACCTACATTT-3′) and shCEP170#2 (5′-GCTGGAGAACTTCATCAAGAA-3′), along with a scrambled control shRNA (5′-TTCTCCGAACGTGTCACGT-3′). These constructs were subsequently cloned and inserted into the pLKO.1-puro vector (Addgene, Watertown, USA) and transfected at 1 μg per 1×10^6 cells, with stable knockdown established via puromycin selection (2 μg/ml, 7 days). Transient transfection efficiency was evaluated at 48 h posttransfection via qPCR/Western blot analysis.

Immunoblot assay

The cell samples were separated by 10% SDS-PAGE; sequentially, the total proteins were transferred onto PVDF membranes (Millipore, Burlington, USA). The membranes were subsequently blocked with 5% dry milk and incubated with antibodies against CEP170 (1:500, ab72505), Twist1 (1:1000, ab50887), galectin-3 (1:500, ab76245), PDGF (1:1000, ab178439), VEGF (1:500, ab291246), and beta-actin (1:3000, ab8226), all purchased from Abcam (Cambridge, UK). The membranes were treated with HRP-labeled secondary antibodies. Each blot was then visualized via an ECL kit (MedChemExpress, Shanghai, China).

Quantitative polymerase chain reaction (qPCR)

Tissue and cellular RNA were extracted with TRIzol reagent (Takara, Kyoto, Japan) and then reverse transcribed into cDNA with an RT Reagent Kit (Takara). A quantitative PCR assay was performed with SYBR II (Takara). The sequences of primers used were as follows: CEP170: forward: 5′-ACAGTACCCCAGGGAA GGTAA-3′, reverse: 5′-ATCCCCAGCAAGTCTTGAGTT-3′; TWIST1: forward: 5′-GTCCGCAGTCTTACGAGGA G-3′, reverse: 5′-GCTTGAGGGTCTGAATCTTGCT-3′; galectin-3: forward: 5′-CTTATTAACCTGCCTTTGCCT GG-3′, reverse: 5′-GCAACATCATTCCCTCTTTGGA-3′; and GAPDH: forward: 5′-TGTGGGCATCAATGGATTTG G-3′, reverse: 5′-ACACCATGTATTCCGGGTCAAT-3′.

Cell viability assays

CCK-8 Assay: Cells were seeded in 96-well plates at a density of 3×10^3 cells/well in 100 μl complete medium and cultured for 24 h. After treatment, 10 μl of CCK-8 reagent (Dojindo, Kumamoto, Japan) was added to each well and incubated for 2 h at 37 °C. The absorbance at 450 nm was measured via a microplate reader (Bio-Rad, Hercules, USA).

EdU Assay: Cells were seeded in 24-well plates and cultured for 24 h. Subsequently, the cells were incubated with 10 μM EdU reagent (BeyoClick™, Wuhan, China) for 2 h at 37 °C, fixed with 4% PFA, and stained. Fluorescence images were captured via a Zeiss Axio Observer microscope (Zeiss, Jena, Germany).

Platelet experiments

Platelet experiments were performed using cryopreserved human platelets (CP10, HemaCare, Los Angeles, USA). Thawed platelets (2×10^8/ml in Tyrode's buffer) were cocultured with 786-O cells (1:200 ratio) for 2 h at 37 °C.

Immunofluorescence assays

The cells were fixed with 4% PFA for 15 min at room temperature, permeabilized with 0.1% Triton X-100 for 10 min, and blocked with 5% BSA for 1 h at 25 °C. The samples were then incubated overnight at 4 °C with primary antibodies against CD41 (1:200, ab134131, Abcam) and GM130 (1:500, ab52649, Abcam). After being washed with PBS, the cells were incubated with Alexa Fluor 488/594-conjugated secondary antibodies (1:1000, A11088/A11012, Invitrogen, Carlsbad, USA) for 1 h at 25 °C. Nuclei were counterstained with DAPI (D9542, Sigma, Darmstadt, Germany) for 5 min. Images were acquired via a confocal microscope (LSM 900, Zeiss) with identical exposure settings across samples.

ELISAs

The levels of TXB2 (ab133054, Abcam) and ATP (ab113849, Abcam) in the culture media of platelet-786-O cell coculture media were quantified via ELISA kits according to the manufacturer's instructions. Briefly, after 2 h of coculture, the supernatants were centrifuged (300×g, 10 min, 4 °C), and 100 μl aliquots were analyzed in duplicate. For TXB2, the samples were incubated with primary antibody (1 h, RT), followed by incubation with HRP-conjugated antibody (1 h) and TMB substrate (15 min), and the absorbance was measured. ATP levels were determined by luminescence after the addition of luciferase reagent.

Transwell migration or invasion assays

For the migration assays, 1×10^5 786-O cells in serum-free DMEM were seeded into the upper chambers of Transwell inserts (8 μm pores, Corning, Corning, USA). The lower chambers contained DMEM supplemented

with 10% FBS. After 24 h of incubation at 37 °C/5% CO_2, non-migrated cells were removed with cotton swabs, and migrated cells on the underside of the membrane were fixed (4% PFA, 15 min), stained with 0.1% crystal violet (20 min), and counted in five random fields (100 × magnification). For invasion assays, inserts were precoated with Matrigel (1:3 dilution in serum-free DMEM, 100 µl/insert) and incubated for 1 h at 37 °C prior to cell seeding.

ATP measurement

The culture media of the cells were placed on ice and processed within 15 min to prevent ATP degradation. ATP quantification was performed via an ATP Assay Kit (ab113849, Abcam), and luminescence was measured via a GloMax Explorer system (Promega, Madison, USA). Values were normalized to total protein in the corresponding cell lysates (BCA assay) for extracellular measurements and to cell counts (determined by hemocytometer) for intracellular measurements.

Tube formation assay

HUVECs (5×10^4 cells/well) were seeded onto growth factor-reduced Matrigel (356231, Corning) in 24-well plates and treated with 500 µl of conditioned medium collected from 786-O cells cultured in serum-free DMEM for 24 h at 37 °C (reaching ∼80% confluence). The conditioned medium was centrifuged, filtered, and stored at −80 °C until use. After 6 h of incubation, the tube networks were imaged via a Nikon Eclipse Ti microscope (4 × objective), and the tube length and branch points were quantified using the Angiogenesis Analyzer plugin of ImageJ (v1.53, Bethesda, USA) by analyzing three random fields per well. The controls included VEGF (50 ng/ml) and serum-free DMEM.

In vivo tumor growth assay

To assess the effect of CEP170 on tumor growth *in vivo*, ccRCC cells were subcutaneously injected into the flanks of nude mice. For subcutaneous tumor xenografts, 5×10^6 786-O cells suspended in 100 µl of PBS:Matrigel (1:1 v/v, Corning 356234) were injected into the right flank of 6-week-old male BALB/c nude mice ($n = 6$/group) under isoflurane anesthesia. The tumor dimensions were measured every 4 days via calipers, and the tumor volume was calculated. Upon reaching the ethical endpoint (day 20 or a tumor volume ⩽1,500 mm^3), the mice were euthanized by CO_2 asphyxiation followed by cervical dislocation. Excised tumors were processed for snap-freezing in liquid nitrogen (Western blot analysis/qPCR). After 20 days of treatment with the indicated interventions, the mice were euthanized, and the tumors were excised. Tumor volume and weight were recorded, and a comparison was made between the control and CEP170 depletion groups to evaluate the impact of CEP170 knockdown on ccRCC tumor growth.

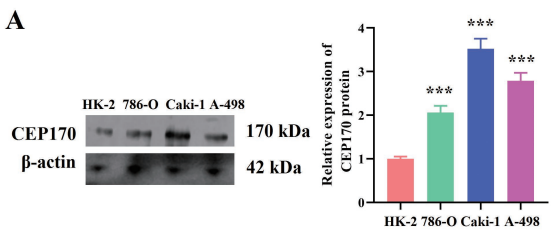

Fig. 1 CEP170 highly expressed in ccRCC cell lines. Immunoblot analysis revealed the expression of CEP170 in the normal renal cell line HK-2 and three ccRCC cell lines: 786-O, CaKi-1, and A-498. Each experiment was repeated 3 times. *** $p < 0.001$ vs. HK-2.

Statistical analysis

Statistical analyses were performed via GraphPad Prism 8.0. The data are presented as the means ± SDs. Multiple group comparisons were analyzed by one-way ANOVA with Tukey's post hoc test. Tumor growth curves were evaluated via two-way repeated-measures ANOVA. Pearson correlation analysis was used to assess relationships between variables. $p < 0.05$ was considered statistically significant.

RESULTS

CEP170 highly expressed in ccRCC tissues

Immunoblotting revealed higher CEP170 expression in ccRCC cell lines (786-O, CaKi-1, and A-498) compared with the normal HK-2 cell line (Fig. 1), indicating that CEP170 is highly expressed in ccRCC.

CEP170 depletion inhibiting the growth of ccRCC cells

To investigate the role of CEP170 in ccRCC cells, we manipulated its expression in 786-O cells via shRNAs and overexpression plasmids. Transfection with the CEP170 overexpression plasmid resulted in a marked increase in CEP170 expression, whereas transfection with the shRNA plasmid led to a significant decrease in CEP170 expression in 786-O cells (Fig. 2A). CCK-8 assays revealed that silencing CEP170 decreased the viability of 786-O cells, whereas CEP170 overexpression increased cell viability (Fig. 2B). Similarly, EdU assays revealed that CEP170 knockdown inhibited 786-O cell growth, whereas CEP170 overexpression promoted cell proliferation (Fig. 2C,D). Therefore, knocking down CEP170 inhibits the proliferation of ccRCC cells.

Suppression of platelet aggregation induced by ccRCC cells through CEP170 knockdown

We next examined the effects of CEP170 on platelet aggregation induced by ccRCC cells. 786-O cells were cocultured with human platelets, and immunostaining

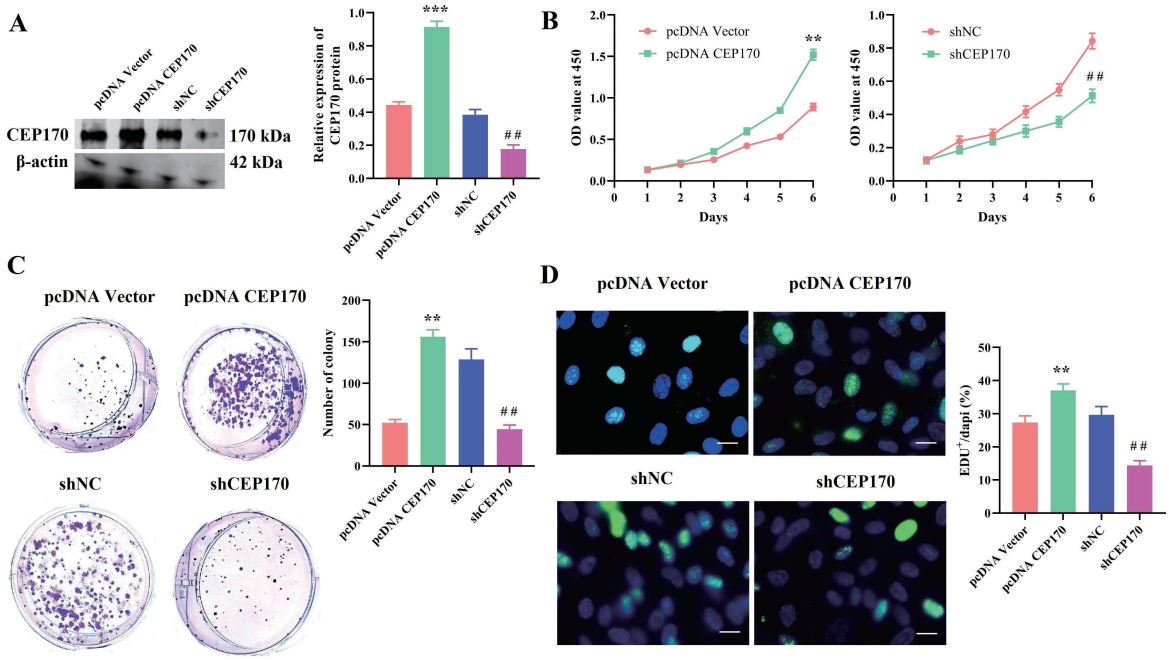

Fig. 2 CEP170 depletion inhibiting the growth of ccRCC cells. (A) CEP170 expression in 786-O cells following the indicated transfections, demonstrated by immunoblot analysis. (B) Growth of 786-O cells after the indicated transfections, assessed by CCK-8 assays with OD450 values measured over a 6-day period. (C) Proliferation of 786-O cells following the indicated transfections, evaluated by EdU assays and (D) Number of EdU-positive cells per field. Each experiment was repeated 3 times. Scale bar, 50 μm. ** $p < 0.01$, *** $p < 0.001$, pcDNA3.1-CEP170 vs. pcDNA3.1-vector, ## $p < 0.01$, shCEP170 vs. shNC. NC, negative control.

assays were performed to detect the platelet aggregation marker CD41. We observed elevated CD41 expression in CEP170-overexpressing 786-O cells, whereas CD41 expression was significantly reduced in CEP170-depleted cells (Fig. 3A). In line with these results, ELISA revealed that the production of the platelet aggregation markers GPIb-IX and GPIIb was increased in the culture media of CEP170-overexpressing 786-O cells cocultured with platelets, whereas their expression was decreased in CEP170-depleted cells, indicating a reduction in platelet aggregation (Fig. 3B). Additionally, ELISA analysis of the TXB2 levels in the culture media of 786-O cells cocultured with platelets confirmed that CEP170 knockdown inhibited platelet aggregation (Fig. 3C). ATP levels, a measure of platelet activation, were also greater in the culture media of CEP170-overexpressing cells than in that of CEP170-depleted 786-O cells cocultured with platelets (Fig. 3D). These results collectively demonstrate that the knockdown of CEP170 inhibits platelet aggregation stimulated by ccRCC cells.

CEp170 knockdown inhibiting angiogenesis and motility in ccRCC cells

Transwell assays revealed that CEP170 overexpression enhanced the motility of 786-O cells, whereas CEP170 depletion significantly reduced cell motility (Fig. 4A,B). Additionally, tube formation assays revealed that CEP170 overexpression in 786-O cells increased the angiogenic potential of HUVECs (Fig. 4C,D). In contrast, CEP170 depletion in 786-O cells suppressed angiogenesis in HUVECs (Fig. 4C,D). Furthermore, the expression of PDGF and VEGF was measured in HUVECs treated with conditioned medium from CEP170-overexpressing 786-O cells. CEP170 depletion led to reduced expression levels of the angiogenesis-related factors PDGF and VEGF (Fig. 4E), whereas CEP170 overexpression increased the expression of these factors (Fig. 4E). Therefore, CEP170 knockdown inhibits both angiogenesis and motility in ccRCC cells.

CEP170 contribution to the Twist1/galectin-3 axis in ccRCC cells

To investigate the underlying mechanism, we performed immunoblot assays and found that overexpression of CEP170 in 786-O cells led to increased levels of Twist1 and galectin-3, whereas depletion of CEP170 reduced the expression of both Twist1 and galectin-3, indicating suppression of the Twist1/galectin-3 axis (Fig. 5A). Similarly, qPCR confirmed that CEP170 regulates the mRNA expression of Twist1 as well

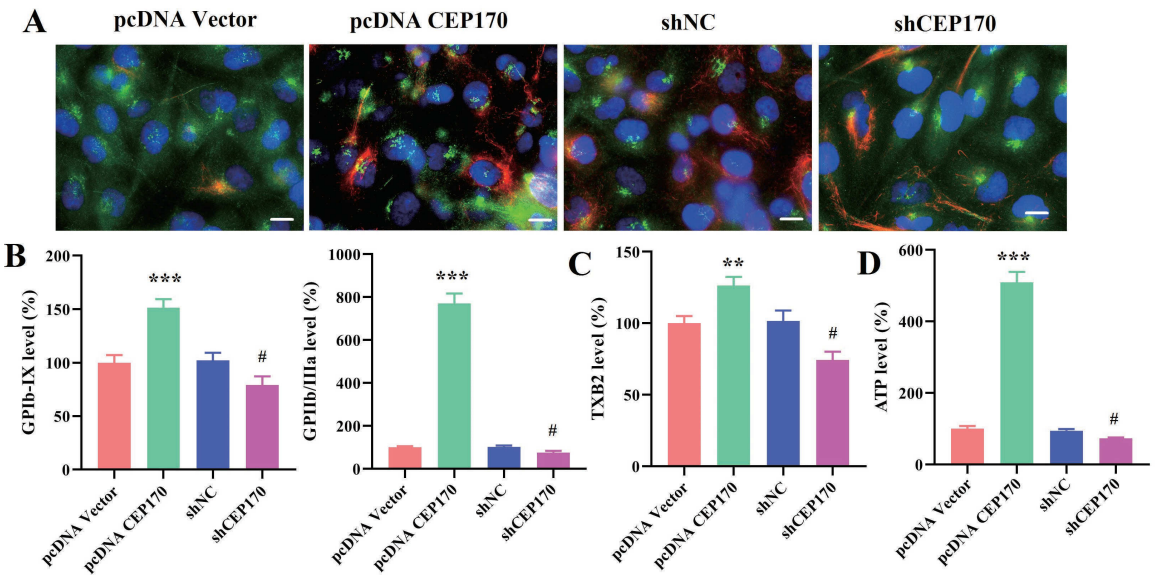

Fig. 3 CEP170 depletion inhibiting the aggregation of platelets from ccRCC cells. (A) Immunofluorescence analysis of CD41 expression in 786-O cells cocultured with platelets following the indicated transfections. Red staining, CD41; green staining, GM130. Scale bar, 30 µm. (B) GPIb-IX and GPIIb/IIIa levels in the culture media of 786-O cells cocultured with platelets after the indicated transfections, assessed by ELISA with OD450 values measured over a 6-day period. (C) TXB2 levels in the culture media of 786-O cells cocultured with platelets following the indicated transfections, evaluated by ELISA. (D) ATP levels in the culture media of 786-O cells cocultured with platelets following the indicated transfections, measured by ELISA. Each experiment was repeated 3 times. ** $p < 0.01$, *** $p < 0.001$, pcDNA3.1-CEP170 vs. pcDNA3.1-vector, ## $p < 0.01$, shCEP170 vs. shNC. NC, negative control.

as galectin-3 in 786-O cells (Fig. 5B). These findings collectively suggest that CEP170 promotes the Twist1/galectin-3 axis in ccRCC.

Suppression of ccRCC growth *in vivo* by CEP170 depletion

To assess the effect of CEP170 on ccRCC tumor growth *in vivo*, shRNAs targeting CEP170 were transfected into 786-O cells to knock down CEP170 expression. CEP170-depleted 786-O cells were then subcutaneously injected into the abdomens of nude mice. After 20 days, we observed a significant reduction in tumor growth in the CEP170-depleted group, with both a smaller tumor volume and lower tumor weight than the control (Fig. 6A). The efficiency of CEP170 silencing in 786-O cells is shown in Fig. 6B. Additionally, CEP170 depletion led to decreased expression levels of Twist1 as well as galectin-3 in tumor tissues (Fig. 6B). These results confirm that CEP170 contributes to ccRCC growth *in vivo*.

DISCUSSION

ccRCC treatment primarily involves a comprehensive approach tailored to individual patient needs [2]. Targeted therapy has emerged as one of the most promising strategies for treating advanced ccRCC, but a deeper understanding of its mechanisms and the identification of novel therapeutic targets are essential for improving treatment outcomes [12]. The abnormal coagulation markers observed in ccRCC patients suggest the presence of a coagulation disorder, which plays a significant role in the progression and metastasis of ccRCC [13]. Platelets contribute to the survival and spread of tumor cells through their interaction with circulating tumor cells, which enhances metastasis [14]. The interaction between tumor cells and platelets, facilitated by physical contact and mutual activation, leads to the formation of TCIPA [15]. This process not only supports immune evasion but also promotes the adhesion and invasion of tumor cells within blood vessels. Additionally, tumor-induced platelets release soluble factors that increase tumor cell invasiveness [15]. In this study, we demonstrated that silencing CEP170 effectively inhibited platelet aggregation induced by ccRCC cells, thereby suppressing ccRCC progression and metastasis. We propose that CEP170 may promote platelet aggregation through Twist1-mediated upregulation of tumor adhesion molecules and/or galectin-3-dependent platelet activation, which is consistent with the known roles of this axis in thrombotic pathways. Future studies should characterize the specific surface factors and secreted mediators underlying this pro-aggregatory phenotype.

Angiogenesis plays a crucial role in the progression

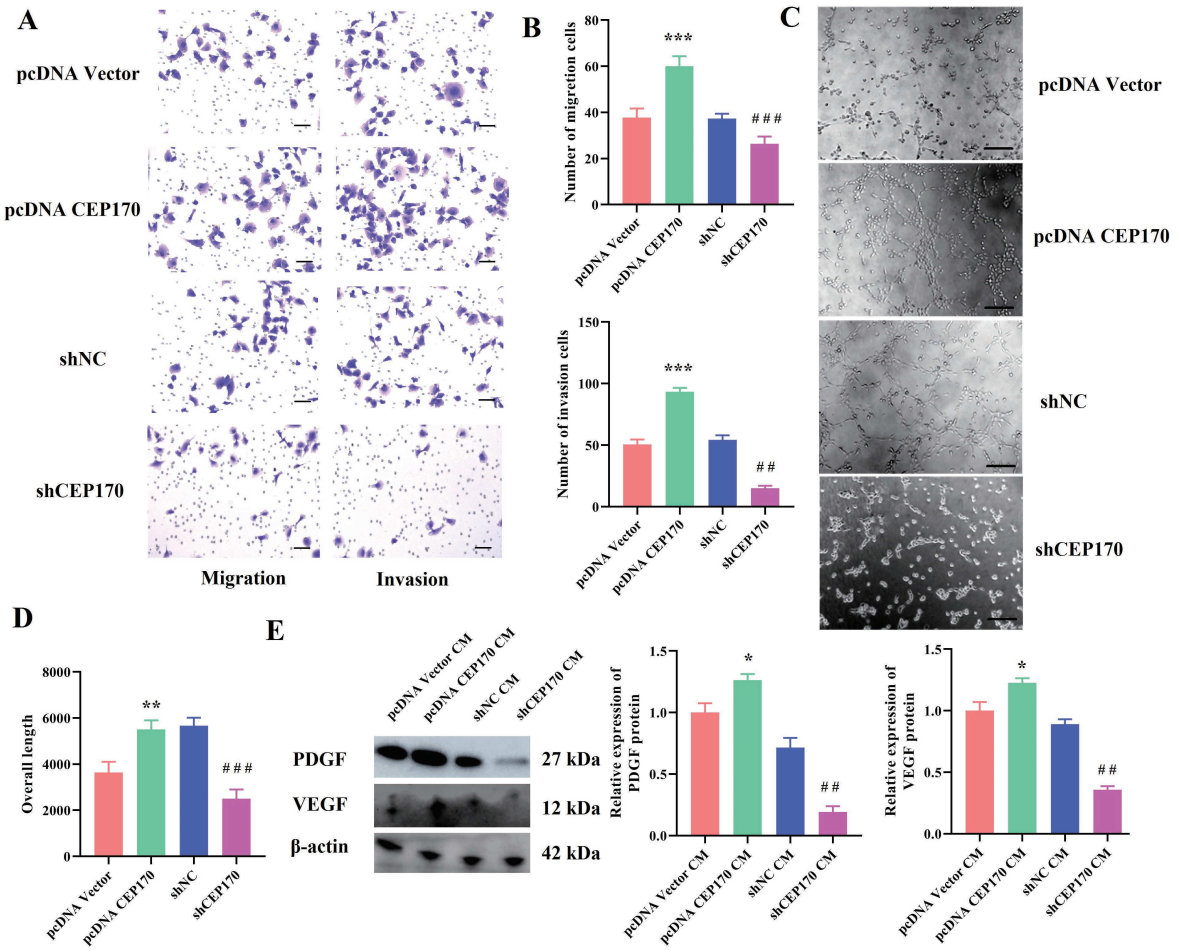

Fig. 4 Migration and angiogenesis induced by ccRCC cells, suppressed by CEP170 depletion. (A) The effects of CEP170 on the migration and invasion of 786-O cells, assessed by transwell assays. Scale bar, 50 μm. (B) Quantification of the data in panel A, where the numbers of migrating and invading cells were counted. (C) The effects of CEP170 in 786-O cells on the angiogenesis of HUVECs, evaluated by tube formation assays. Scale bar, 300 μm. (D) Quantification of the data in panel C, with the number of branch points counted. (E) Immunoblot analysis of PDGF and VEGF expression in HUVECs after the indicated transfections in 786-O cells. Each experiment was repeated 3 times. * $p < 0.05$, ** $p < 0.01$, *** $p < 0.001$, pcDNA3.1-CEP170 vs. pcDNA3.1-vector, ## $p < 0.01$, ### $p < 0.001$, shCEP170 vs. shNC. NC, negative control.

of ccRCC, representing a complex biological process that involves numerous molecules [16]. Understanding the roles and interactions of these molecules, as well as gaining deeper insight into the biological mechanisms of ccRCC angiogenesis, could lead to new strategies and therapeutic approaches for treating ccRCC [17]. Key processes in angiogenesis, such as endothelial cell proliferation and directional migration, are critical for tumor vascularization [17]. In this study, we demonstrated that silencing CEP170 inhibits both the angiogenesis and migration of ccRCC cells, suggesting that CEP170 is a pivotal regulator of ccRCC angiogenesis. The CEP170-Twist1/galectin-3 axis in tumor cells likely upregulates PDGF/VEGF secretion through Twist1-mediated transcriptional activation and galectin-3-enhanced mRNA stability, creating a proangiogenic microenvironment.

CEP170 is a highly conserved nucleolar protein that plays a critical role in cellular processes, particularly during mitosis, where it is involved in chromosome condensation [18]. It has been shown to interact with key signaling pathways, including the p53/CP-1 axis, contributing to the regulation of immune responses and tumor progression [19]. As a crucial factor in cell cycle regulation, CEP170 also influences the invasiveness and metastatic potential of tumor cells [19]. Given its involvement in various cellular functions, understanding the relationship between CEP170 expression and ccRCC progression is highly important for developing targeted therapeutic strategies [19]. In our

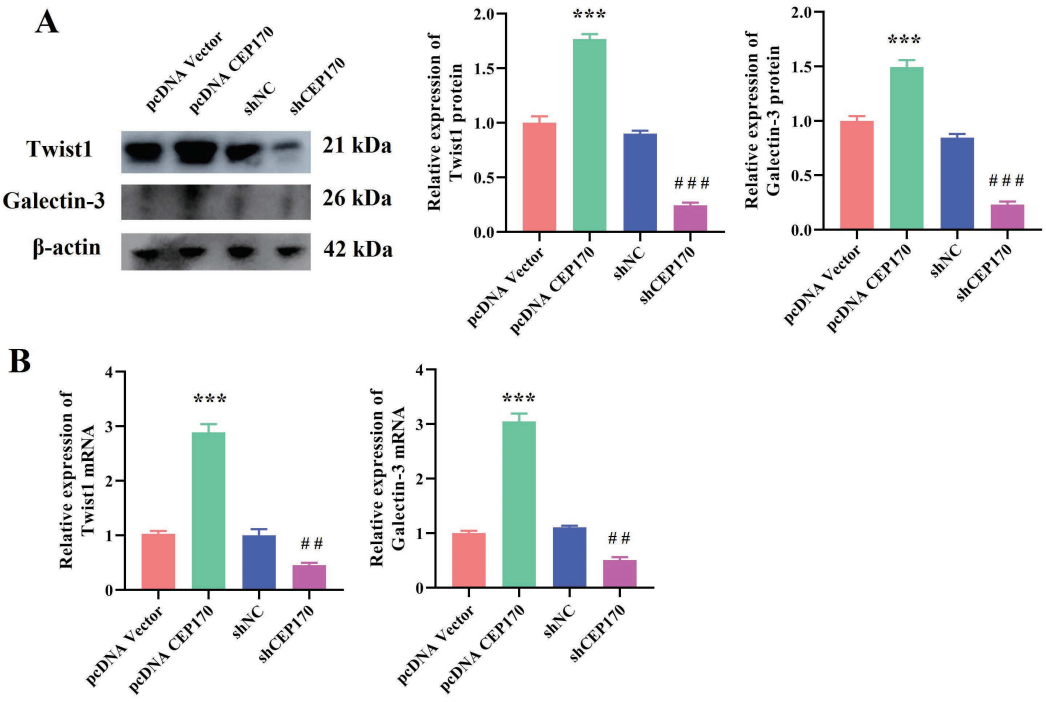

Fig. 5 CEP170 contribution to the Twist1/galectin-3 axis in ccRCC cells. (A) Immunoblot analysis of Twist1 and galectin-3 expression in 786-O cells following the indicated transfections. (B) mRNA levels of Twist1 and galectin-3 in 786-O cells after the indicated transfections, measured by qPCR assays. Each experiment was repeated 3 times. ** $p < 0.01$, *** $p < 0.001$, pcDNA3.1-CEP170 vs pcDNA3.1-vector; # $p < 0.05$, ## $p < 0.01$, ### $p < 0.001$, shCEP170 vs. shNC. NC, negative control.

study, we confirmed the elevated expression of CEP170 in ccRCC and demonstrated that its overexpression facilitates multiple processes, such as platelet aggregation and angiogenesis, which collectively contribute to ccRCC progression. These findings highlight the potential of targeting CEP170 as a novel approach in ccRCC treatment.

Galectin-3, a multifunctional proto-oncoprotein, plays a pivotal role in regulating various tumorigenic processes, including cell proliferation, invasion, angiogenesis, and apoptosis [20]. It has emerged as a potential biomarker for tumor metastasis and a promising target for cancer therapy [21]. TWIST1, an upregulated interstitial marker in dormant ccRCC cells, is strongly associated with ccRCC progression. The transcription factor Twist1 influences key aspects of ccRCC biology. Twist1 can bind to the promoter of the proto-oncogene AKT2, driving its expression, which in turn activates YB-1, a protein linked to cell proliferation, ultimately promoting tumor cell growth [22]. Our study demonstrated that CEP170 modulates platelet aggregation, angiogenesis, cell motility, and tumor growth in ccRCC through the Twist1/galectin-3 axis. We propose that CEP170 may regulate the Twist1/galectin-3 axis by facilitating Twist1 nuclear localization and enhancing galectin-3 secretion, as supported by their coordinated expression changes in our experiments. This dual regulation could drive ccRCC progression through both transcriptional and secretory pathways.

While this study highlights the role of CEP170 in ccRCC progression through the Twist1/galectin-3 axis, it has several limitations. First, our findings are primarily based on *in vitro* cell experiments and mouse models. Although these initial results suggest that CEP170 plays a significant role in ccRCC, further validation in clinical samples is needed to confirm its clinical relevance. Second, while we demonstrated the impact of CEP170 on tumor cell proliferation, migration, platelet aggregation, and angiogenesis, the precise molecular mechanisms underlying its regulation of the Twist1/galectin-3 axis remain unclear. Future studies should focus on elucidating the downstream signaling pathways and other molecular interactions involved in CEP170 regulation. Galectin-3 can activate multiple intracellular signaling pathways [20]. Our results demonstrate that CEP170 knockdown simultaneously reduces galectin-3 expression and platelet aggregation, which is consistent with this known mechanism.

The identification of CEP170 as a key regulator of ccRCC progression through platelet aggregation and angiogenesis suggests its potential as a novel therapeutic target. While this study focused on elucidating the mechanistic basis of the oncogenic function of CEP170, these findings lay the groundwork for future transla-

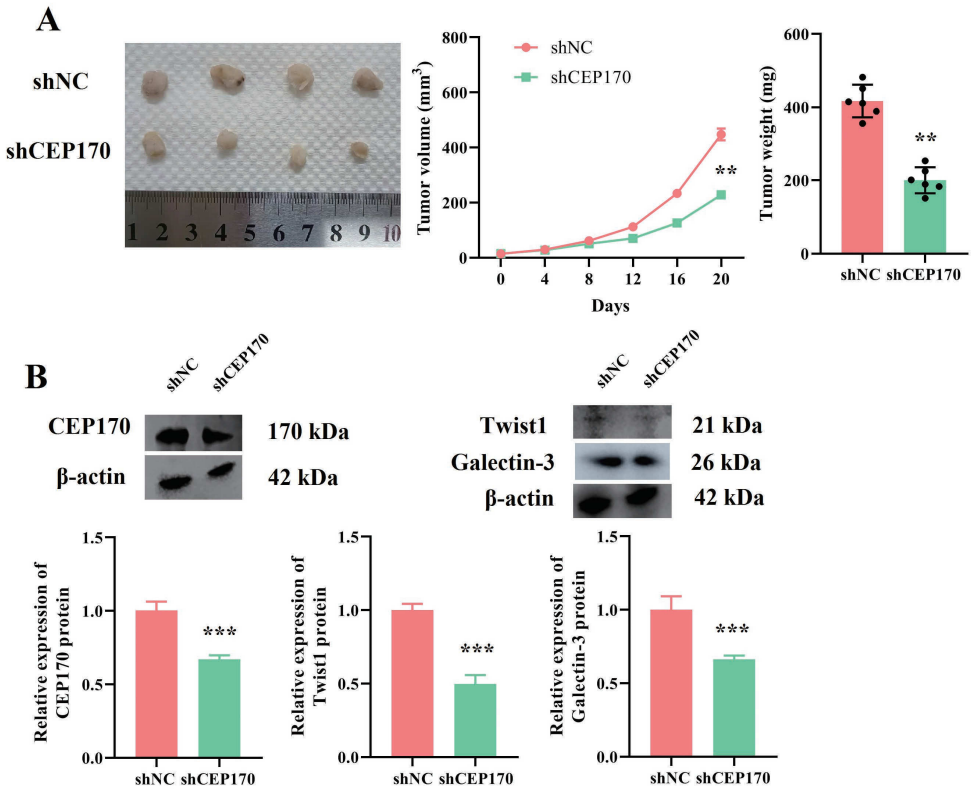

Fig. 6 Suppression of ccRCC growth *in vivo* by CEP170 ablation. (A) Impact of CEP170 on ccRCC growth *in vivo* ($n = 6$ per group), evaluated by tumor growth assays. Representative images of the tumors are shown (left), and the tumor volume was measured every 4 days until day 20. Tumor weight was also assessed at the end of the experiment. (B) Expression of CEP170 (left), Twist1 and galectin-3 (right) in tumor tissues from different experimental groups, shown by immunoblot analysis. ** $p < 0.01$, *** $p < 0.001$, shCEP170 vs. shNC. NC, negative control.

tional investigations. The centrosomal localization and structural features of CEP170 may offer unique opportunities for targeted intervention, particularly in combination with existing antiangiogenic therapies. Furthermore, the association between CEP170 expression and aggressive tumor phenotypes warrants exploration of its utility as a prognostic biomarker. Future studies should explore direct targeting strategies, including small molecule inhibitors or protein-protein interaction disruptors, as well as evaluate the therapeutic window of CEP170 modulation in preclinical models. These efforts may ultimately lead to new therapeutic avenues for ccRCC patients, particularly those resistant to current standard therapies.

Moreover, despite the promising potential of CEP170 as a novel target for ccRCC therapy, specific therapeutic strategies targeting CEP170 have yet to be developed. Future research could explore the development of selective inhibitors or antibodies against CEP170 and evaluate their therapeutic efficacy in ccRCC treatment. Additionally, investigating the relationship between CEP170 and the ccRCC microenvironment—particularly its interactions with immune cells, angiogenesis, and platelet aggregation—will provide a more comprehensive understanding of its role in ccRCC progression and help refine therapeutic approaches. In addition, a key limitation is our primary reliance on the 786-O cell line, which may not fully represent the heterogeneity of ccRCC; future studies should validate these findings in additional models and primary patient samples.

CONCLUSION

In summary, we demonstrated that CEP170 is highly expressed in ccRCC cell lines and promotes platelet aggregation as well as angiogenesis potentially via Twist1/galectin-3 axis. Our findings suggest that CEP170 could serve as a potential therapeutic target for ccRCC.

REFERENCES

1. Soupir AC, Hayes MT, Peak TC, Ospina O, Chakiryan NH, Berglund AE, Stewart PA, Nguyen J, et al (2024) Increased spatial coupling of integrin and collagen IV in the immunoresistant clear-cell renal-cell carcinoma tumor microenvironment. *Genome Biol* **25**, 308.

2. Li Z, Xin S, Huang L, Tian Y, Chen W, Liu X, Ye B, Bai R, et al (2025) BEX4 inhibits the progression of clear cell renal cell carcinoma by stabilizing SH2D4A, which is achieved by blocking SIRT2 activity. *Oncogene* **44**, 665–678.
3. Yang X, Han B, Xie Q, Li Y, Li Q, Hu X, Zhao H, Xu X (2025) Low expression of mitochondrial ribosomal protein S5 is associated with poor prognosis in patients with clear cell renal cell carcinoma. *Appl Immunohistochem Mol Morphol* **33**, 22–28.
4. Gali KV, Rai GD, Choudhary A, Surag KR, Kamath GS, Chawla A, Gunashekar V (2024) Retrograde aortic dissection encountered amidst nephrectomy for renal cell carcinoma with IVC thrombus: A case report. *BMC Urol* **24**, 264.
5. Soytas M, Dragomir A, Sawaya GBN, Hesswani C, Tanguay M, Finelli A, Wood L, Rendon R, et al (2025) Is there a minimum percentage of sarcomatoid component required to affect outcomes of localised renal cell carcinoma? *BJU Int* **135**, 818–827.
6. Yang B, Zheng Y, Zheng MQ, Wang D, Ren SQ, Tian JZ (2024) Partial nephrectomy versus radiofrequency ablation in patients with cT1a renal cell carcinoma: A surveillance, epidemiology, end results (SEER) analysis. *Medicine (Baltimore)* **103**, e40721.
7. Weijman JF, Vuolo L, Shak C, Pugnetti A, Mukhopadhyay AG, Hodgson LR, Heesom KJ, Roberts AJ, et al (2024) Roles for CEP170 in cilia function and dynein-2 assembly. *J Cell Sci* **137**, jcs261816.
8. Xu X, Wang K, Vera O, Verma A, Jasani N, Bok I, Elemento O, Du D, et al (2022) Gain of chromosome 1q perturbs a competitive endogenous RNA network to promote melanoma metastasis. *Cancer Res* **82**, 3016–3031.
9. Wei R, Cui X, Min J, Lin Z, Zhou Y, Guo M, An X, Liu H, et al (2022) NAT10 promotes cell proliferation by acetylating CEP170 mRNA to enhance translation efficiency in multiple myeloma. *Acta Pharm Sin B* **12**, 3313–3325.
10. Conduit SE, Pearce W, Bhamra A, Bilanges B, Bozal-Basterra L, Foukas LC, Cobbaut M, Castillo SD, et al (2024) A class I PI3K signalling network regulates primary cilia disassembly in normal physiology and disease. *Nat Commun* **15**, 7181.
11. Singh K, Tantravahi U, Lomme MM, Pasquariello T, Steinhoff M, Sung CJ (2016) Updated 2013 College of American Pathologists/American Society of Clinical Oncology (CAP/ASCO) guideline recommendations for human epidermal growth factor receptor 2 (HER2) fluorescent *in situ* hybridization (FISH) testing increase HER2 positive and HER2 equivocal breast cancer cases; retrospective study of HER2 FISH results of 836 invasive breast cancers. *Breast Cancer Res Treat* **157**, 405–411.
12. Yojiro I, Takaya Y, Rei U, Noriyoshi T, Kazuya T, Yu S, Keiichi J (2022) Chronic expanding hematoma of the left erector spinae muscle after stereotactic body radiotherapy for renal cell carcinoma: A case report. *J Med Case Rep* **16**, 353.
13. Tullemans BME, Brouns SLN, Swieringa F, Sabrkhany S, van den Berkmortel FWPJ, Peters NAJB, de Bruijn P, Koolen SLW, et al (2022) Quantitative and qualitative changes in platelet traits of sunitinib-treated patients with renal cell carcinoma in relation to circulating sunitinib levels: A proof-of-concept study. *BMC Cancer* **22**, 653.
14. Tullemans BME, Nagy M, Sabrkhany S, Griffioen AW, Egbrink MGAO, Aarts M, Heemskerk JWM, Kuijpers MJE (2018) Tyrosine kinase inhibitor Pazopanib inhibits platelet procoagulant activity in renal cell carcinoma patients. *Front Cardiovasc Med* **5**, 142.
15. Sabrkhany S, Griffioen AW, Pineda S, Sanders L, Mattheij N, van Geffen JP, Aarts MJ, Heemskerk JWM, et al (2016) Sunitinib uptake inhibits platelet function in cancer patients. *Eur J Cancer* **66**, 47–54.
16. Vaeteewoottacharn K, Kariya R, Saisomboon S, Paungpan N, Luang S, Piyawattanamatha N, Kitkhuandee A, Okada S (2024) Lenalidomide suppresses VEGF-dependent angiogenesis and cholangiocarcinoma growth in an *in vivo* mouse model. *ScienceAsia* **50**, ID 2024111.
17. Khaleel S, Perera M, Papa N, Kuo F, Golkaram M, Rappold P, Kotecha RR, Coleman J, et al (2025) Gene expression of prostate-specific membrane antigen (FOLH1) in clear cell renal cell carcinoma predicts angiogenesis and response to tyrosine kinase inhibitors. *Urol Oncol* **43**, 192.e21–192.e28.
18. Omolaoye TS, Omolaoye VA, Kandasamy RK, Hachim MY, Du Plessis SS (2022) Omics and male infertility: Highlighting the application of transcriptomic data. *Life (Basel)* **12**, 280.
19. Ma D, Wang F, Wang R, Hu Y, Chen Z, Huang N, Tian Y, Xia Y, et al (2022) α-/γ-Taxilin are required for centriolar subdistal appendage assembly and microtubule organization. *Elife* **11**, e73252.
20. Syn G, Lee YQ, Lim ZY, Chan GC (2024) Galectin-3: action and clinical utility in chronic kidney disease. *Int Urol Nephrol* **56**, 3535–3543.
21. Ghodsieh K, Reza H, Mohammad R, Hamid S, Hoda S, Mohammad Ebrahim S, Davoud J (2024) Galectin-3 marker expression in renal cell carcinoma and correlation with patient's clinicopathologic factors: A cross-sectional study. *Caspian J Intern Med* **16**, 165–168.
22. Wang H, Gao Y, Guo F, Zhou P, Ma Z, Chi K, Ye J, Sun H, et al (2024) ERβ-regulated circATP2B1/miR-204-3p/TWIST1 positive feedback loop facilitates epithelial to mesenchymal transition in clear cell renal cell carcinoma. *Transl Oncol* **51**, 102213.